Cranfield

College of Aeronautics Report 8412
April 1984

Another Look at the Use of Complex Sources for the Generation of Bodies of Revolution in Incompressible Flow

by P.A.T. Christopher and H.D. Wealthy

College of Aeronautics
Cranfield Institute of Technology
Cranfield, Bedford, U.K.

Cranfield
College of Aeronautics Report 8412
April 1984

Another Look at the Use of Complex Sources for the Generation of Bodies of Revolution in Incompressible Flow

by P.A.T. Christopher and H.D. Wealthy

College of Aeronautics
Cranfield Institute of Technology
Cranfield, Bedford, U.K.

ISBN 0 947767 01 0

£7.50

"The views expressed herein are those of the authors alone and do not necessarily represent those of the Institute."

Summary

It is shown that by the use of discrete axial distributions of imaginary source discs it is possible to generate a wide class of axi-symmetric bodies. In particular thin bodies with bluff ends may be obtained, as well as a variety of other shapes. These results, which were obtained by an "indirect" method, indicate that a re-formulation as a "direct" method is possible and this is being pursued.

1. Introduction

In an earlier paper, Ref.1, the method of complex sources, for generating axi-symmetric bodies in incompressible flow, was re-introduced. This technique was originally suggested by Bateman in Refs. 3 and 4 and, subsequently and independently by Armstrong in Ref. 5.

The work described in Ref. 1 was aimed first at a re-capitulation of the basic method, as given by Armstrong, stressing the simplicity of the potential, stream-function and velocity relations, and second at an extension of the method to thin, missile-like bodies, particularly those with bluff ends. It was hoped to develop an "indirect" technique for generating such bodies which would, ultimately, lend itself to re-formulation as a "direct" method.

In Ref. 1 several examples were shown in order to illustrate some possibilities of the indirect method, and these included thin bodies with very bluff ends. However, it was concluded that more work was required before a systematic indirect technique could be obtained. This method required to be such that it permitted a relatively simple and controlled shaping of the body, particularly at the ends. Further, the method had to be capable of being turned into a direct one by means of imposition of the known body boundary conditions.

The present paper describes further research on this problem in which the use of discrete distributions of imaginary source discs is explored.

2. Linear Distribution of Imaginary Sources (Imaginary Source Disc Type A)

Before proceeding with our main aim, we need to return to Sections 3.1 and 3.3 of Ref. 1 in order to rectify a shortcoming. If, as before,

we take a distribution

$$g(\eta) = g_1\eta \ , \ (-\eta_1 \leqslant \eta \leqslant \eta_1), \tag{2.1}$$

which we will define as corresponding to an imaginary source disc of Type A, this produces a stream function, at a point P(x,r),

$$\psi_s(x,r) = -\frac{g_1}{4\pi}\int_{\eta_1}^{\eta_1}\frac{i(x-i\eta)}{R(x,r,\eta)}\,d\eta \tag{2.2}$$

Expanding the integral, we have

$$\int\frac{i(x-i\eta)\eta}{R(x,r,\eta)}\,d\eta = ix\int\frac{\eta d\eta}{R(x,r,\eta)} + \int\frac{\eta^2 d\eta}{R(x,r,\eta)} \ ,$$

which, upon use of the integral $I_1(m = 1,2)$ from Appendix 1 of Ref. 1, gives

$$\int\frac{i(x-i\eta)\eta}{R(x,r,\eta)}d\eta = -\tfrac{1}{2}\{(\eta-ix)R(x,r,\eta) - r^2I_b\} \ , \tag{2.3}$$

where

$$I_b = \int\frac{d\eta}{R(x,r,\eta)} \ . \tag{2.4}$$

If now we substitute from (2.3) into (2.2) we get

$$4\pi\psi_s(x,r) = \tfrac{1}{2}g_1\Big[(\eta-ix)R(x,r,\eta) - r^2I_b\Big]_{-\eta_1}^{\eta_1}$$

$$= \tfrac{1}{2}g_1\{(\eta_1-ix)R(x,r,\eta_1) + (\eta_1+ix)R(x,r,-\eta_1) - r^2\Big[I_b(\eta_1) - I_b(-\eta_1)\Big]\} \ .$$

Now, as shown in Ref. 1, page 30,

$$(\eta_1-ix)R(x,r,\eta_1) + (\eta_1+ix)R(x,r,-\eta_1) = 2\rho\sigma\mathrm{Cos}(\omega+\gamma) \ , \tag{2.5}$$

where

$$\rho = \{(x^2+r^2-\eta_1^2)^2 + 4x^2\eta_1^2\}^{\frac{1}{4}} ,$$

$$\sigma = (x^2+\eta_1^2)^{\frac{1}{2}} ,$$

$$\text{Sin } 2\omega = 2x\eta_1/\rho^2 , \quad \text{Cos } 2\omega = (x^2+r^2-\eta_1^2)/\rho^2 ,$$

$$\text{Sin } \gamma = x/\sigma \quad , \quad \text{Cos } \gamma = \eta_1/\sigma .$$

Thus

$$4\pi\psi_s(x,r) = g_1\{\rho\sigma\text{Cos}(\omega+\gamma) - \tfrac{1}{2}r^2\left[I_b(\eta_1) - I_b(-\eta_1)\right]\} \qquad (2.6)$$

In order to determine $\psi_s(x,r)$ in (2.6) we need to obtain an expression for I_b, and, in Ref. 1 this was done by reference to the table of integrals, Ref. 2, page 81, item 2.261. In the notation of Ref. 2

$$R(x,r,\eta) = (c\eta^2 + b\eta + a)^{\frac{1}{2}} ,$$

with

$$c = -1 , \quad b = -2ix , \quad a = x^2 + r^2$$

and

$$\Delta = 4ac - b^2 = -4r^2 .$$

Since $c < 0$, $\Delta < 0$, then the appropriate form of the integral is, apparently, the third of the alternative forms given, which is

$$I_b = -\text{Sin}^{-1}\{\frac{-\eta - ix}{r}\} = \text{Sin}^{-1}\{\frac{\eta + ix}{r}\} \qquad (2.7)$$

It follows that

$$I_b(\eta_1) - I_b(-\eta_1) = \text{Sin}^{-1}(\frac{\eta_1+ix}{r}) - \text{Sin}^{-1}(\frac{-\eta_1+ix}{r})$$

which, by use of the identity

$$\text{Sin}^{-1}z_1 \pm \text{Sin}^{-1}z_2 = \text{Sin}^{-1}\{z_1(1-z_2^2)^{\frac{1}{2}} \pm z_2(1-z_1^2)^{\frac{1}{2}}\} ,$$

can be written as

$$\mathrm{Sin}^{-1}\{\frac{2\rho\sigma}{r^2}\,\mathrm{Cos}(\omega+\gamma)\}\ .$$

Substitution into (2.6) then gives

$$4\pi\psi_s(x,r) = g_1\{\rho\sigma\mathrm{Cos}(\omega+\gamma) - \tfrac{1}{2}r^2\mathrm{Sin}^{-1}[\frac{2\rho\sigma}{r^2}\,\mathrm{Cos}(\omega+\gamma)]\} \qquad (2.8)$$

Examination of the second term in (2.8) shows that it can only be meaningful if

$$-1 \leq \frac{2\rho\sigma}{r^2}\,\mathrm{Cos}(\omega+\gamma) \leq 1 \qquad (2.9)$$

and, therefore, raises the question of the validity of (2.8). Let us check this by first determining the shape of the stagnation streamline for certain cases. The total stream function is given by

$$\psi = \tfrac{1}{2}Ur^2 + \psi_s\ , \qquad (2.10)$$

and the equation of the stagnation streamline, $\psi = 0$, becomes

$$-\tfrac{1}{2}Ur^2 = \psi_s$$

or

$$\frac{4\pi Ur2}{g_1} = F(x,r) = F_1 + F_2\ , \qquad (2.11)$$

where

$$\left.\begin{aligned} F_1 &= -2\rho\sigma\mathrm{Cos}(\omega+\gamma) \\ \text{and} \\ F_2 &= r^2\mathrm{Sin}^{-1}[\frac{2\rho\sigma}{r^2}\,\mathrm{Cos}(\omega+\gamma)] \end{aligned}\right\} \qquad (2.12)$$

Fixing a point x_f, r_f on this streamline then gives, as in Ref. 1,

$$r^2 = h(x_f,r_f,\eta_1)F(x,r,\eta_1)\ , \qquad (2.13)$$

where

$$h(x_f,r_f,\eta_1) = r_f^2/F(x_f,r_f,\eta_1) \qquad (2.14)$$

and

$$F(x_f,r_f,\eta_1) = -2\rho_f\sigma_f \cos(\omega_f + \gamma_f) + r_f^2 \sin^{-1}\{\frac{2\rho_f\sigma_f}{r_f^2} \cos(\omega_f + \gamma_f)\} \tag{2.15}$$

Some numerical solutions of (2.13) have been obtained by iteration. This was done by re-writing (2.13) in the form

$$G(x,r,\eta_1) = h(x_f,r_f,\eta_1)F(x,r,\eta) - r^2 = 0 = H(x,r,\eta_1) - r^2 = 0 \tag{2.16}$$

and employing the approximate Newton-Raphson algorithm

$$x_{n+1} = x_n - G_n/G_n' \quad , \tag{2.17}$$

where

$$G_n' = \frac{dG}{dx} \simeq \frac{G_n - G_{n-1}}{x_n - x_{n-1}} = \frac{H_n - H_{n-1}}{x_n - x_{n-1}} = H_n' \ . \tag{2.18}$$

The cases taken were

$x_f = 0$, $r_f = 0.1$,

with

$\eta_1 = 0.08$, 0.09 and 0.099.

The oblate bodies generated are shown in Fig. 1 and correspond exactly with those obtained by the use of the transformation of equation (3.12) of Ref. 1, i.e. they are oblate spheroids of a family spanning the range between a flat disc ($\eta_1 \to r(x=0)$) and a sphere ($\eta_1 \to 0$). This has, therefore, demonstrated that, for the numerical values chosen, the inequality (2.9) is, apparently, satisfied, i.e. the $\psi = 0$ streamline lies in a region of the x,r space for which condition (2.9) is met.

If we were interested, only, in the generation of oblate spheroids the use of (2.8) might well prove to be satisfactory for all cases, in the sense that the $\psi = 0$ streamline lies in the domain defined by (2.9). On the other hand we may be interested in taking a number of distributions of the type described by (2.1) and distributing these along the x (or ξ) axis, with a view to generating thin bodies with blunt ends. Such a procedure would almost certainly require a knowledge of the value of ψ_s at more distant positions from the origin of the individual distributions and certainly require us to know whether condition (2.9) is violated in some parts of the flow field. The validity of (2.9) may be readily checked by first noting that

$$\frac{2\rho\sigma}{r}\,\mathrm{Cos}(\omega+\gamma) = \frac{\sqrt{2}}{r^2}\{\eta_1(\rho^2+x^2+r^2-\eta_1^2)^{\frac{1}{2}} - x(\rho^2-x^2-r^2+\eta_1^2)^{\frac{1}{2}}\}\ , \qquad (2.19)$$

which upon squaring gives

$$\begin{aligned}\{\frac{2\rho\sigma}{r^2}\,\mathrm{Cos}(\omega+\gamma)\}^2 &= \frac{2}{r^4}\{\eta_1^2\,(\rho^2+x^2+r^2-\eta_1^2) + x^2(\rho^2-x^2-r^2+\eta_1^2)\\ &\quad - 2x\eta_1(\rho^2+x^2+r^2-\eta_1^2)^{\frac{1}{2}}(\rho^2-x^2-r^2+\eta_1^2)^{\frac{1}{2}}\}\\ &= \frac{2}{r^4}\{\eta_1^2(\rho^2+x^2+r^2-\eta_1^2) + x^2(\rho^2-x^2-r^2+\eta_1^2)\\ &\quad - 2x\eta_1\left[\rho^4-(x^2+r^2-\eta_1^2)^2\right]^{\frac{1}{2}}\}\\ &= \frac{2}{r^4}\{\eta_1^2(\rho^2+x^2+r^2-\eta_1^2) + x^2(\rho^2-x^2-r^2+\eta_1^2) - 4x^2\eta_1^2\}\\ &= \frac{2}{r^4}\{\eta_1^2(\rho^2-x^2+r^2-\eta_1^2) + x^2(\rho^2-x^2-r^2-\eta_1^2)\}\ , \qquad (2.20)\end{aligned}$$

and observing that (2.9) corresponds to the condition

$$0 \leqslant \{\frac{2\rho\sigma}{r^2}\,\mathrm{Cos}(\omega+\gamma)\}^2 \leqslant 1 \qquad (2.21)$$

Utilizing (2.20), and taking

$r = 0.08$, $\eta_1 = 0.09$

with x various, it is not difficult to show that for values of $x > 20$ the value of

$$\{\frac{2\rho\sigma}{r^2}\,\mathrm{Cos}(\omega+\gamma)\}^2 < 0\ ,$$

implying that (2.21) is violated. As a result it is clear that we require an expression for I_b which has a general validity for all points of the flow field. This we will now develop.

3. An Alternative Form for I_b.

Recapitulating, we have, from Appendix 1 of Ref. 1, that

$$I_b = \int \frac{d\eta}{R(x,r,\eta)}$$

where

$$R(x,r,\eta) = (c\eta^2 + b\eta + a)^{\frac{1}{2}}$$

and

$$c = -1, \quad b = -2ix, \quad a = x^2+r^2, \quad \Delta = -4r^2.$$

However, we may re-write this integral in the form

$$I_b = i\int \frac{d\eta}{i(c\eta^2+b\eta+a)^{\frac{1}{2}}} = i\int \frac{d\eta}{(-c\eta^2-b^2-a)^{\frac{1}{2}}} = i\int \frac{d\eta}{(\eta^2+2ix\eta-x^2-r^2)^{\frac{1}{2}}}, \qquad (3.1)$$

which is in the first of the alternative forms given in Ref. 2, page 81, item 2.261 and is given by

$$\begin{aligned} I_b &= i\ln\{2(\eta^2+2ix\eta-x^2-r^2)^{\frac{1}{2}} + 2\eta + 2ix\} \\ &= i\ln\{2i(x^2-2ix\eta-\eta^2+r^2)^{\frac{1}{2}} + 2(\eta+ix)\} \\ &= i\ln\{2iR(x,r,\eta) + 2(\eta+ix)\} \end{aligned} \qquad (3.2)$$

It follows that

$$\begin{aligned} \int_{-\eta_1}^{\eta_1} \frac{d\eta}{R(x,r,\eta)} &= I_b(\eta_1) - I_b(-\eta_1) \\ &= i\left[\ln\{2iR(x,r,\eta) + 2(\eta+ix)\}\right]_{-\eta_1}^{\eta_1} \\ &= i\{\ln(2i\rho e^{-i\omega} + 2\sigma e^{i\gamma}) - \ln(2i\rho e^{i\omega} - 2\sigma e^{-i\gamma})\} \\ &= i\ln\left(\frac{i\rho e^{-i\omega} + \sigma e^{i\gamma}}{i\rho e^{i\omega} - \sigma e^{-i\gamma}}\right) \\ &= i\ln\left\{\frac{i\rho(\mathrm{Cos}\omega - i\mathrm{Sin}\omega) + \sigma(\mathrm{Cos}\gamma + i\mathrm{Sin}\gamma)}{i\rho(\mathrm{Cos}\omega + i\mathrm{Sin}\omega) - \sigma(\mathrm{Cos}\gamma - i\mathrm{Sin}\gamma)}\right\} \\ &= i\ln\left(-\frac{\beta e^{i\tau}}{\beta e^{-i\tau}}\right) = i\ln(-e^{2i\tau}) \\ &= i\{\ln(-1) + \ln(e^{2i\tau})\} = i\{-\pi i + 2i\tau\} = -(2\tau-\pi), \end{aligned} \qquad (3.3)$$

where

$$\beta = \{(\rho\mathrm{Sin}\omega+\sigma\mathrm{Cos}\gamma)^2 + (\rho\mathrm{Cos}\omega+\sigma\mathrm{Sin}\gamma)^2\}^{\frac{1}{2}} \qquad (3.4)$$

and

$$\tau = \mathrm{Tan}^{-1}\left\{\frac{\rho\mathrm{Cos}\omega+\sigma\mathrm{Sin}\gamma}{\rho\mathrm{Sin}\omega+\sigma\mathrm{Cos}\gamma}\right\} \qquad (3.5)$$

Note. The choice of $\ln(-1) = -\pi i$ in (3.3) is not obvious but was found to be appropriate in numerical calculations.

Substitution into (2.6) then gives

$$4\pi\psi_s(x,r) = g_1\{\rho\sigma\mathrm{Cos}(\omega+\gamma) + \tfrac{1}{2}r^2(2\tau-\pi)\}. \qquad (3.6)$$

The solution for the $\psi = 0$ streamline may be obtained as before, using (2.13) and (2.14), but with

$$\left.\begin{aligned} F_1 &= -2\rho\sigma\mathrm{Cos}(\omega+\gamma) \\ F_2 &= -r^2(2\tau-\pi) \end{aligned}\right\} \qquad (3.7)$$

Computations were performed for the cases shown in Fig. 1 and these agree exactly with those obtained using the expressions for F_1, F_2 given in (2.12)

Having rectified this shortcoming in the expression for ψ_s for a Type A source disc, we may return to our main aim of seeking to generate body shapes using axial distributions of imaginary source discs.

4. Constant Distribution of Imaginary Sources (Imaginary Source Disc Type B)

For convenience we recapitulate the results for the constant distribution of imaginary sources

$$g(\eta) = g_o\eta/|\eta| \ , \quad (-\eta_1 \leq \eta \leq \eta_1) \qquad (4.1)$$

which we now define as corresponding to an imaginary source disc of Type A. From Ref. 1, Section 3.2, we have

$$\psi_s(x,r) = -\frac{ig_o}{4\pi}\int_{-\eta_1}^{\eta_1}\frac{(x-i\eta)\,\eta\,d\eta}{R(x,r,\eta)\,|\eta|} \qquad (4.2)$$

which gives

$$\psi_s(x,r) = \frac{g_o}{2\pi}\{\rho\mathrm{Cos}\omega - \rho(\eta_1=0)\} \ , \qquad (4.3)$$

where ρ, ω are defined in Section 2.

The total stream function is, therefore,

$$\psi(x,r) = \tfrac{1}{2}Ur^2 + \frac{g_o}{2\pi}\{\rho\mathrm{Cos}\omega - \rho(\eta_1=0)\} \tag{4.4}$$

and the stagnation streamline, $\psi = 0$, is given by

$$\frac{\pi Ur^2}{g_o} = \rho(\eta_1=0) - \rho\mathrm{Cos}\omega \tag{4.5}$$

5. Axial Distributions of Imaginary Source Discs - Stream Function Formulation.

We consider now a discrete axial distribution of imaginary source discs. That is imaginary source discs, described by

$$g_j(\eta_j) \quad , \quad (-\eta_{1j} < \eta < \eta_{1j}),$$

are placed at discrete points $x = \xi_j$ on the proposed body axis. See Fig. 3.

The stream function at x,r for a single type B source disc, of strength $g_{o_j}\,\mathrm{Sign}(\eta)$, located at ξ_j is

$$\psi_s(x,r) = \frac{g_{oj}}{2\pi}\{\rho_j\mathrm{Cos}\omega_j - \rho_j(\eta_j=0)\} \quad , \tag{5.1}$$

where

$$\rho_j = \left[\{(x-\xi_j)^2 + r^2 - \eta_{1_j}^2\}^2 + 4(x-\xi_j)^2\eta_{1_j}^2\right]^{\frac{1}{4}} \tag{5.2}$$

and

$$\mathrm{Cos}2\omega_j = \{(x-\xi_j)^2 + r^2 - \eta_{1_j}^2\} \div \rho_j^2 \quad , \tag{5.3}$$

which are obvious generalizations of the expressions, for the case $\xi_j = 0$, given in Section 2. Using linear superposition, a discrete distribution of n Type B source discs produces a stream function at x,r of

$$\psi_{s_B}(x,r) = \frac{1}{2\pi}\sum_{j=1}^{n} g_{o_j}\{\rho_j\mathrm{Cos}\omega_j - \rho_j(\eta_j=0)\} \tag{5.4}$$

In a similar way a discrete distribution of m type A source discs, of strength $g_{1_k}\eta$, located at ξ_k produces a stream function of

$$\psi_{S_A}(x,r) = \frac{1}{4\pi} \sum_{k=1}^{m} g_{1_k}\{\rho_k\sigma_k \mathrm{Cos}(\omega_k+\gamma_k) + \tfrac{1}{2}r^2(2\tau_k-\pi)\} \ , \tag{5.5}$$

where ρ_k, $\mathrm{Cos}2\omega_k$ have similar forms to (5.2) and (5.3),

$$\sigma_k = \{(x-\xi_k)^2 + \eta_{1_k}^2\}^{\frac{1}{2}} \ , \tag{5.6}$$

$$\left.\begin{aligned} \mathrm{Sin}\gamma_k &= (x-\xi_k)/\sigma_k \\ \mathrm{Cos}\gamma_k &= \eta_{1_k}/\sigma_k \end{aligned}\right\} \tag{5.7}$$

and

$$\tau_k = \mathrm{Tan}^{-1}\left\{\frac{\rho_k \mathrm{Cos}\omega_k + \sigma_k \mathrm{Sin}\gamma_k}{\rho_k \mathrm{Sin}\omega_k + \sigma_k \mathrm{Cos}\gamma_k}\right\} \tag{5.8}$$

Adding the various stream functions then produces a total stream function

$$\psi(x,r) = \tfrac{1}{2}Ur^2 + \psi_{S_A}(x,r) + \psi_{S_B}(x,r) \tag{5.9}$$

and an equation defining the stagnation streamline, $\psi = 0$, which is

$$r^2 = -\frac{1}{2U}\{\psi_{S_A}(x,r) + \psi_{S_B}(x,r)\} = F(x,r) \tag{5.10}$$

6. Some Bodies Generated by Discrete Axial Distributions of Type A and B Source Discs.

In Ref. 1 body shapes generated by single Type A and Type B source discs were explored, as well as bodies arising from combinations of these. Other bodies were generated by means of conjugate imaginary source pairs on a specified surface = (ξ). See Ref. 1, Section 4. We shall now demonstrate some of the range of bodies that may be generated by discrete axial distributions of Type A and Type B source discs using the expressions developed in Section 5. In so doing it is hoped to obtain some insight into the flexibility of the method and the extent to which controlled shaping of the body is possible.

The computations described in Ref. 1 never specified the strengths g_o or g_1, since the manner in which the stagnation streamline was determined did not require it. However, for the multi-discrete distributions we are

now using, and bearing in mind the ultimate goal of a direct method, this procedure has to be modified and all the g_{o_j} and g_{1_k} will have to be specified. Thus we may solve (5.10) by means of a fixed point iteration, where x and all the strength coefficients g_{o_j} and g_{1_k} are known, to give the value of r at a particular, chosen, value of x. Stepping, in an appropriate manner, along the x-axis then allows a solution for the body shape $r_{Body}(x)$.

As a first step in these numerical exercises, it was decided to determine the magnitudes of g_o, g_1 required to produce bodies whose maximum radius is approximately unity. Thus by taking a single Type B distribution with $\xi = 0$, $\eta_1 = 0.8$ and fixing one point on the stagnation streamline at $x = 0$, $r = 1.0$, then (4.5) or (5.10) may be solved to give $g_o = 2.5\pi U$. Replacing the Type B distribution with a Type A then gives $g_1 = 4.47132\pi U$.

In order to avoid the need to specify the stream velocity U and, thereby, non-dimensionalize the velocity relations given later, it is convenient to define

$$f_o = \frac{g_o}{\pi U} \quad , \quad f_1 = \frac{g_1}{\pi U} \tag{6.1}$$

Thus the values quoted in the paragraph immediately above are $f_o = 2.5$, $f_1 = 4.47132$.

Let us consider a first example of body generation using the Type B source disc defined by $\eta_1 = 0.8$, $f_o = 2.5$ and placing three discs at $\xi = -0.8$, 0 and 0.8, respectively. The resultant shape is shown in Fig. 4 and is encouraging in that the shape is prolate with a nose shape which is blunter than an hemisphere.

Note. As in Figs. 1 and 2 the body generated is symmetrical with respect to both the x and r axes, and only one-quarter of the body is illustrated. This also applies to Figs. 5-10, but not to Fig. 11.

Intuitively we might reasonable expect that if the spacing between the source discs were increased then the body shape would undulate, and this is borne out in Fig. 5.

By returning the spacing to a smaller value we would expect to remove the undulation, and this is demonstrated in Fig. 6.

We have already observed that bodies generated by Type A source discs, in isolation, may be made arbitrarily thin in the x-sense, by allowing η_1 to approach the maximum body radius. See Fig. 1. In contrast to this an isolated Type B disc has a definite lower limit to its thickness in the x-sense, and as η_1 is allowed to approach the maximum radius a cusp develops in the body shape. As a result it is reasonable to think that by placing Type A discs at the extremes, in the x-sense, we might be able to generate bluffer body shapes.

Bearing in mind the results of our first three exercises, two longer bodies were generated, Fig.7. Both bodies used constant f factors and η_1 along their length, but one used Type B discs and the other Type A. As can be seen from Fig. 7 the body generated by Type B discs is smooth, whereas that obtained from Type A discs developed ripples just behind the nose, this nose being considerably blunter than the other. If we take the above Type B distribution and replace the discs at the extremities (i.e. at -10 and 10) with Type A discs we again obtain a bluffer nose. See Fig. 8.

Undulations in the body surface, due to having too large a disc spacing, were shown in Fig. 5. This is demonstrated more dramatically in Fig. 9, which is the body generated by Type B discs having the same strength and η_1 as Fig. 7, but with $\Delta\xi = 0.8$. These ripples may be removed by reducing the disc spacing and/or increasing f_o. See for comparison Fig. 6 where $\Delta\xi = 0.8$, $f_o = 2.5$ and $\eta_1 = 0.8$.

In Fig. 10 the effect of linearly reducing η_1, in order to produce taper, is illustrated. In this the body taper closely follows the reduction of η_1 over the interval $6.0 \leqslant |\xi| \leqslant 9.6$. Some rippling just behind the nose was also evident.

So far the bodies generated have all been symmetrical with respect to both the x and r axes. Provided the influence of the individual source discs is reasonably localised, discs placed on the negative portion of the x-axis should have little effect on the body shape generated about the positive branch of the x-axis, and vice-versa. To check this a body was generated, using a similar distribution to that used in the previous example but with the discs confined to the positive branch of the x-axis only. If we align the stagnation points of Figs. 10 and 11, we obtain correspondence between the body profiles back to about 60 per cent of the body as shown in Fig. 11.

7. Velocity relations.

In order to obtain the pressure distributions over the bodies generated by the imaginary source disc technique we shall, in addition, need velocity relations.

If u_A, v_A are the velocity perturbations induced by an isolated Type A source disc in a uniform stream U, then we have from equations (3.34) and 3.35) of Ref. 1 that

$$u_A = -\frac{g_1}{4\pi}(2\mu - \mathrm{Sin}2\mu) - \frac{g_1}{4\pi r^2}\{\left[\eta_1(1-\frac{r^2}{\rho^2}) - ix\right]R(x,r,\eta_1) + \left[\eta_1(1-\frac{r^2}{\rho^2}) + ix\right]R(x,r,-\eta_1)\} \qquad (7.1)$$

and

$$v_A = \frac{ig_1}{8\pi r}\{1 - \frac{x^2+\eta_1^2+r^2}{\rho^2}\}\left[R(x,r,\eta_1) - R(x,r,-\eta_1)\right] \quad , \qquad (7.2)$$

where μ is defined in equation (3.15) of Ref. 1.
Now the incremental stream function, ψ_{s_A}, produced by this source disc is, from equation (3.6),

$$\psi_{s_A} = \frac{g_1}{8\pi}\{2\rho\sigma\mathrm{Cos}(\omega+\gamma) + r^2(2\tau-\pi)\} \quad , \qquad (7.3)$$

whereas the alternative expression for this quantity is, from equation (3.17) of Ref. 1,

$$\psi_{s_A} = -\frac{g_1 r^2}{8\pi}(2\mu - \mathrm{Sin}2\mu) \qquad (7.4)$$

It follows that

$$2\mu - \mathrm{Sin}2\mu = -\frac{1}{r^2}\{2\rho\sigma\mathrm{Cos}(\omega+\gamma) + r^2(2\tau-\pi)\} \qquad (7.5)$$

Making use of (7.5 and (6.1), together with the relations for ρ,ω and $R(x,r,\eta_1)$, then (7.1) and (7.2) become

$$\frac{u_A}{U} = \frac{f_1}{4r^2}\{2\rho\left[\sigma\mathrm{Cos}(\omega+\gamma) + \eta_1(\frac{r^2}{\rho^2}-1)\mathrm{Cos}\omega + x\mathrm{Sin}\omega\right] + r^2(2\tau-\pi)\} \qquad (7.6)$$

and

$$\frac{v_A}{U} = \frac{f_1\rho}{4r}\{1 - \frac{x^2+r^2+\eta_1^2}{\rho^2}\}\mathrm{Sin}\omega \qquad (7.7)$$

The corresponding expressions for a discrete distribution of Type A source discs, as in Section 5.0, are

$$\frac{u_A}{U} = \sum_{k=1}^{n} \frac{f_{1k}}{4r^2} \{2\rho_k [\sigma_k \mathrm{Cos}(\omega_k+\gamma_k) + \eta_{1k}(\frac{r^2}{\rho^2_k} - 1)\mathrm{Cos}\omega_k + x\mathrm{Sin}\omega_k] + \tau^2(2\tau_k - \pi)\} \qquad (7.8)$$

and

$$\frac{v_A}{U} = \sum_{k=1}^{n} \frac{f_{1k}}{4r} \rho_k \left\{1 - \frac{x^2+r^2+\eta_{1k}}{\rho^2_k}\right\} \mathrm{Sin}\omega_k \qquad (7.9)$$

The incremental stream function, ψ_{s_B}, produced by a Type B source disc is, from (4.3),

$$\psi_{s_B} = \frac{g_o}{2\pi} \{\rho\mathrm{Cos}\omega - \rho(\eta_1=0)\} \quad ,$$

which may be differentiated appropriately to give the corresponding velocity relations defined by

$$u_B = \frac{1}{r}\frac{\partial}{\partial r}(\psi_{s_B}) \quad , \quad v_B = -\frac{1}{r}\frac{\partial}{\partial x}(\psi_{s_B}). \qquad (7.10)$$

Now

$$\frac{\partial}{\partial r}(\psi_{s_B}) = \frac{g_o}{2\pi} \{\frac{\partial \rho}{\partial r}\mathrm{Cos}\omega - \rho\mathrm{Sin}\omega \frac{\partial \omega}{\partial r} - \frac{\partial}{\partial r}\rho(\eta_1=0)\} \qquad (7.11)$$

Also

$$\rho^4 = (x^2+r^2-\eta_1^2)^2 + 4x^2\eta_1^2 \quad ,$$

which, upon differentiation with respect to r, gives

$$4\rho^3\frac{\partial \rho}{\partial r} = 4r(x^2+r^2-\eta_1^2)$$

or

$$\frac{\partial \rho}{\partial r} = \frac{r(x^2+r^2-\eta_1^2)}{\rho^3} \quad , \qquad (7.12)$$

which gives

$$\frac{\partial}{\partial r}\rho(\eta_1=0) = \frac{r}{(x^2+r^2)^{\frac{1}{2}}} \qquad (7.13)$$

In addition,

$$2\omega = \mathrm{Tan}^{-1}\{\frac{2x\,\eta_1}{x^2+r^2-\eta_1^2}\} \quad ,$$

which, upon differentiation with respect to r, gives

$$\frac{\partial\omega}{\partial r} = \frac{\frac{1}{2}}{\{1 + [\frac{2x\,\eta}{x^2+r^2-\eta_1^2}]^2\}} \frac{\partial}{\partial r}\{\frac{2x\eta_1}{x^2+r^2-\eta_1^2}\}$$

or

$$\frac{\partial\omega}{\partial r} = -\frac{2xr\eta_1}{\rho^4} \qquad (7.14)$$

Substituting from (7.12) - (7.14) into (7.11) and (7.10) then gives

$$\frac{u_B}{U} = \tfrac{1}{2}f_o\{(\frac{x^2+r^2-\eta_1^2}{\rho^3})\mathrm{Cos}\omega + \frac{2x\eta_1}{\rho^3}\,\mathrm{Sin}\omega - \frac{1}{(x^2+r^2)^{\frac{1}{2}}} \qquad (7.15)$$

Now

$$\frac{\partial}{\partial x}(\psi s_B) = \frac{g_o}{2\pi}\{\frac{\partial\rho}{\partial x}\mathrm{Cos}\omega - \rho\mathrm{Sin}\omega\frac{\partial\omega}{\partial x} - \frac{\partial}{\partial x}\,\rho(\eta_1=0)\} \quad , \qquad (7.16)$$

whilst

$$\frac{\partial\rho}{\partial x} = \frac{x}{\rho^3}\,(x^2 + r^2 + \eta_1^2) \quad , \qquad (7.17)$$

$$\frac{\partial}{\partial x}\rho(\eta_1=0) = \frac{x}{(x^2+r^2)^{\frac{1}{2}}} \qquad (7.18)$$

and

$$\frac{\partial\omega}{\partial x} = \frac{\eta_1}{\rho^4}\,(r^2 - x^2 - \eta_1^2) \qquad (7.19)$$

Hence

$$\frac{v_B}{U} = -\frac{f_o}{\frac{1}{2}r}\left\{\frac{x(x^2+r^2+\eta_1^2)}{\rho^3}\,\mathrm{Cos}\omega - \frac{\eta_1(r^2-x^2-\eta_1^2)}{\rho^3}\,\mathrm{Sin}\omega - \frac{x}{(x^2+r^2)^{\frac{1}{2}}}\right\} \qquad (7.20)$$

The corresponding expressions for a discrete distribution of Type B source discs are

$$\frac{u_B}{U} = \sum_{j=1}^{m} \tfrac{1}{2} f_{o_j} \left\{ \left(\frac{x^2+r^2-\eta_{1_j}^2}{\rho^3_j} \right) \mathrm{Cos}\omega_j + \frac{2x\eta_{1_j}}{\rho^3_j} \mathrm{Sin}\omega_j - \frac{1}{(x^2+r^2)^{\frac{1}{2}}} \right\} \quad (7.21)$$

and

$$\frac{v_B}{U} = -\sum_{j=1}^{m} \frac{f_{o_j}}{\tfrac{1}{2} r} \left\{ \frac{x(x^2+r^2+\eta_{1_j}^2)}{\rho^3_j} \mathrm{Cos}\omega_j - \frac{\eta_{1_j}(r^2-x^2-\eta_{1_j}^2)}{\rho^3_j} \mathrm{Sin}\omega_j - \frac{x}{(x^2+r^2)^{\frac{1}{2}}} \right\} \quad (7.22)$$

For any finite discrete distribution of Type A and Type B source discs, as envisaged in Sections 5 and 6, the components of the velocity will be

$$\left. \begin{aligned} u_T &= U + u_A + u_B \\ \text{and} \\ v_T &= v_A + v_B \end{aligned} \right\} , \quad (7.23)$$

where u_A, u_B, v_A and v_B are obtained from (7.8), (7.9),(7.21) and (7.22) respectively. The corresponding pressure coefficient is then

$$C_p = 1 - \left(\frac{u_T}{U}\right)^2 - \left(\frac{v_T}{U}\right)^2 . \quad (7.24)$$

8. Discussion and Conclusions.

From the limited number of examples presented in the previous section a number of useful pointers toward the establishment of a 'direct' method have been gained.

Whichever way we express the boundary conditions on the known body shape, i.e. streamline shape or local surface slope, we shall have to satisfy these conditions at a discrete number of points, and this number will determine the number of source discs to be employed. For each disc the value of η_1, the disc radius; ξ , the disc axial position, and f, the non-dimensionalized strength parameter, will have to be determined.

On the basis of the previous examples, particularly those shown in Figs. 7,8,10 and 11, it could be a reasonable strategy to set $\eta_1(\xi)$ as a fixed fraction of the local radius $r_B(\xi)$. Also, they provide a guide to the number, and spacing, of the discs. For parallel sections of the

body a fixed value of $\Delta\xi$ might be used, chosen so as to exclude the situation of Fig. 9, whilst at corners (e.g. cone-cylinder junction) and at body ends, particularly blunt ends, the discs would probably need closer packing in a manner related to the body surface curvature in the meridian plane. With η_1 and ξ thus pre-determined, the discretely fixed boundary conditions then allow a system of simultaneous linear equations in the unknown parameters f_{o_j}, f_{1_k} to be established. Inversion of the system matrix then allows a determination of the f_{o_j}, f_{1_k}.

Implicit in this strategy is the decision as to the type of source disc to use as a building-block for the bodies. On the basis of the previous examples it appears that the Type B is the best choice since it produces smoother body shapes and is simpler to compute. The role of the Type A disc lies in its ability to produce blunter end shapes and sharper corners.

Whether this strategy is successful remains to be seen. More complicated strategies concerning the choice of ξ and $\eta_1(\xi)$ are clearly possible. Work is proceeding on this topic and the aim is to make the method as computationally efficient and economic as possible.

References

1. Christopher, P.A.T. 'The generation of axi-symmetric bodies in incompressible flow by means of distributions of complex sources' College of Aeronautics Report 8304 C.I.T., Cranfield, March (1983)

2. Gradshteyn, I.S. and Ryzhik, I.M. 'Tables of integrals, series and products' Academic Press, (1965)

3. Bateman, H. 'Some Geometrical theorems connected with Laplace's equation and the equation of wave motion' American Journ. Maths. Vol. 34, pp.325-360, (1912)

4. Bateman, H. 'The inertia coefficients of an airship in a frictionless fluid' NACA Report 164, (1923)

5. Armstrong, A.H. 'An extension of the hydrodynamic source-sink method for axi-symmetric bodies' A.R.C. R. & M. 3020, December (1954)

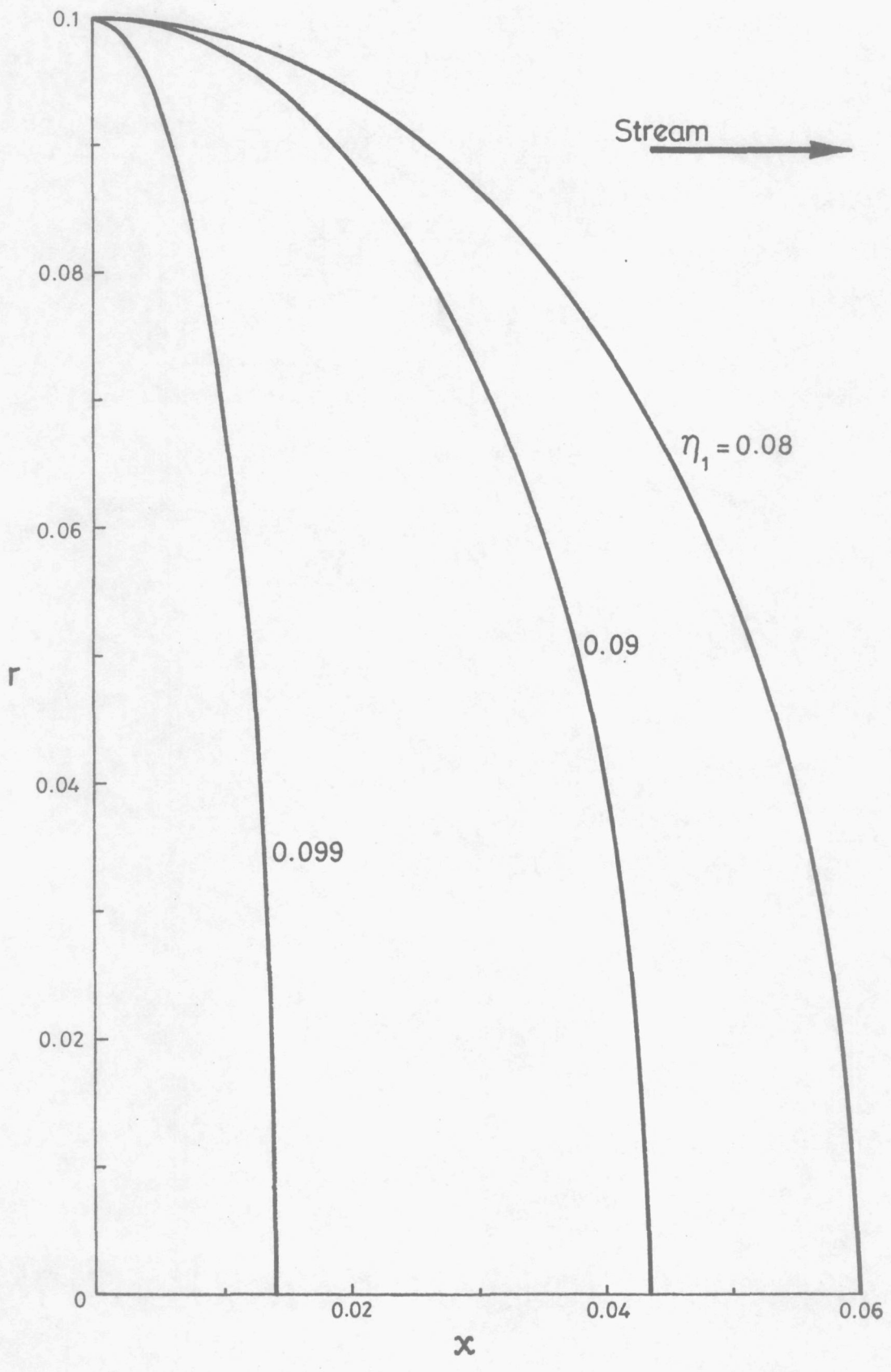

Figure 1. Body shapes produced by an imaginary source disc, type A.

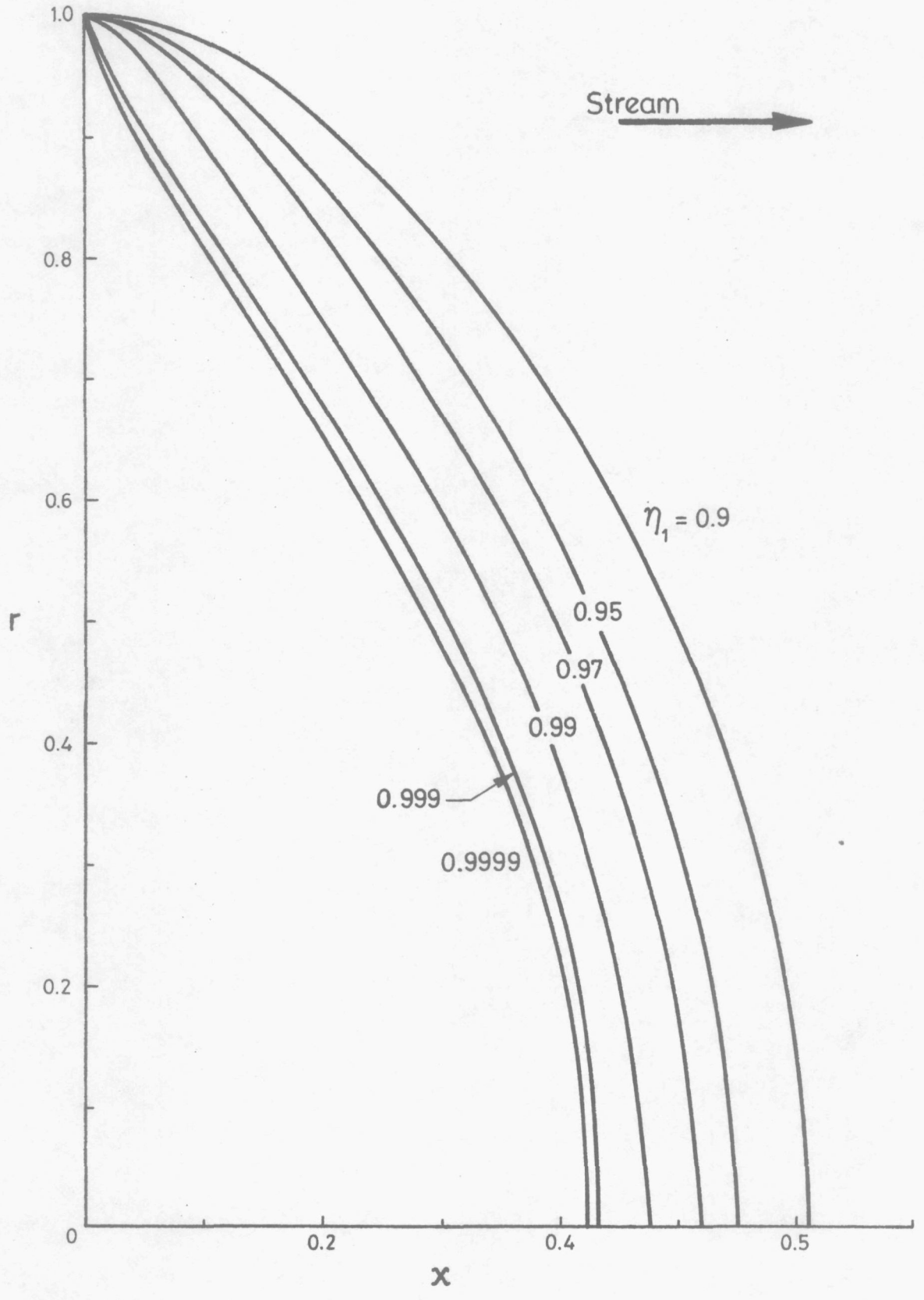

Figure 2. Body shapes produced by an imaginary source disc, type B.

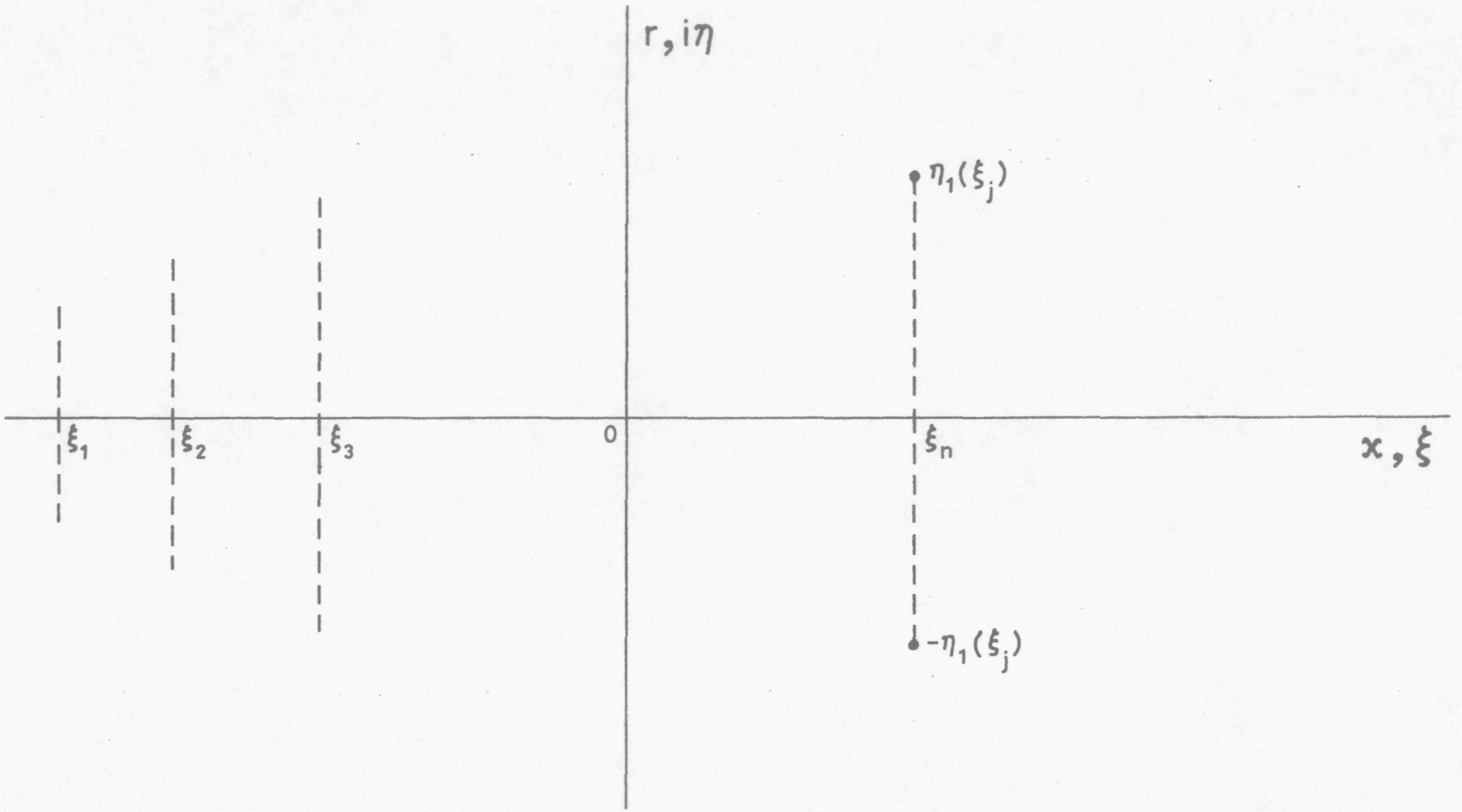

Figure 3. Discrete distribution of imaginary source discs.

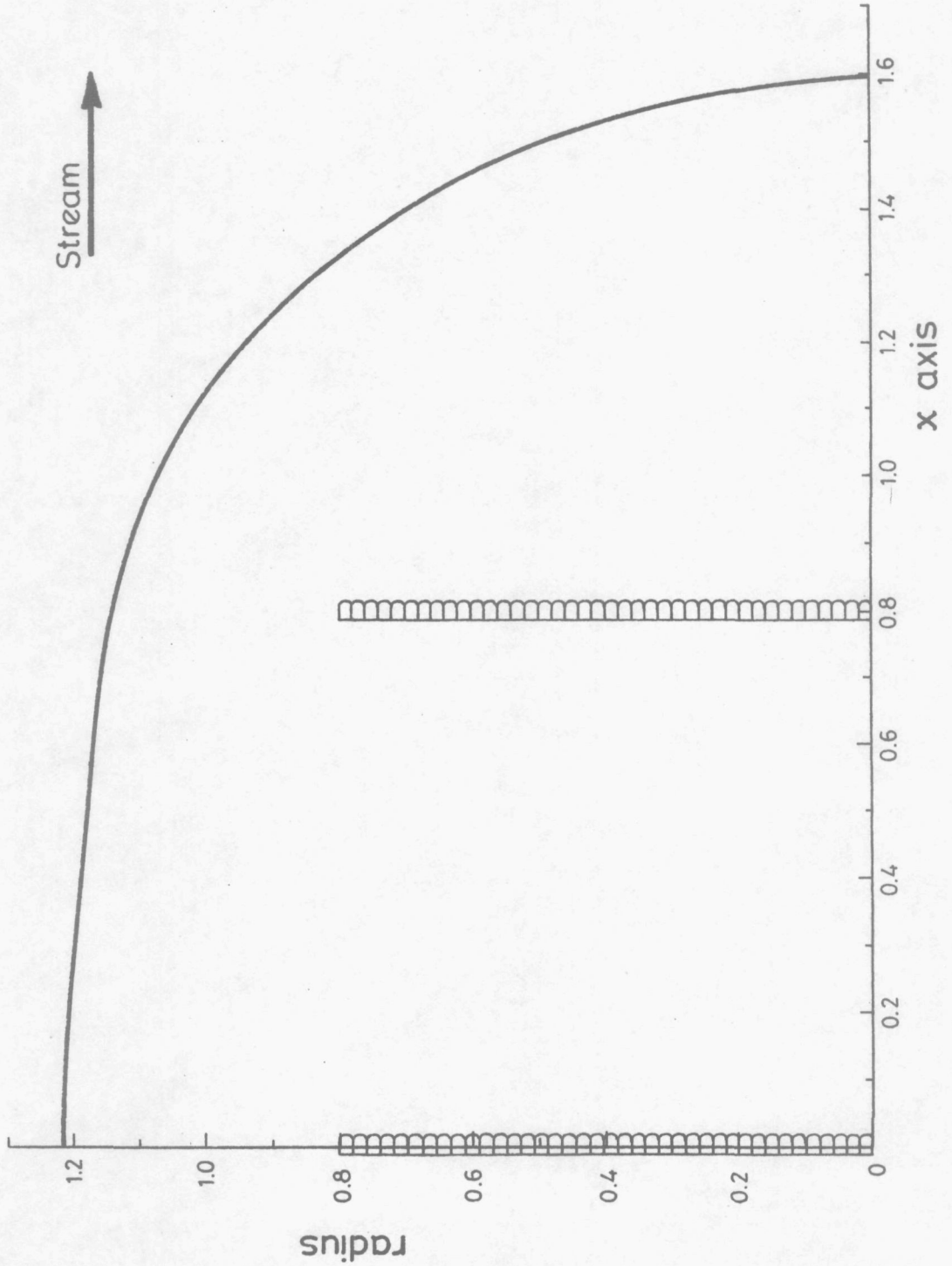

Figure 4. Three type B discs. $\xi = -0.8, 0, 0.8$, $f_o = 2.5$, $\eta_1 = 0.8$.

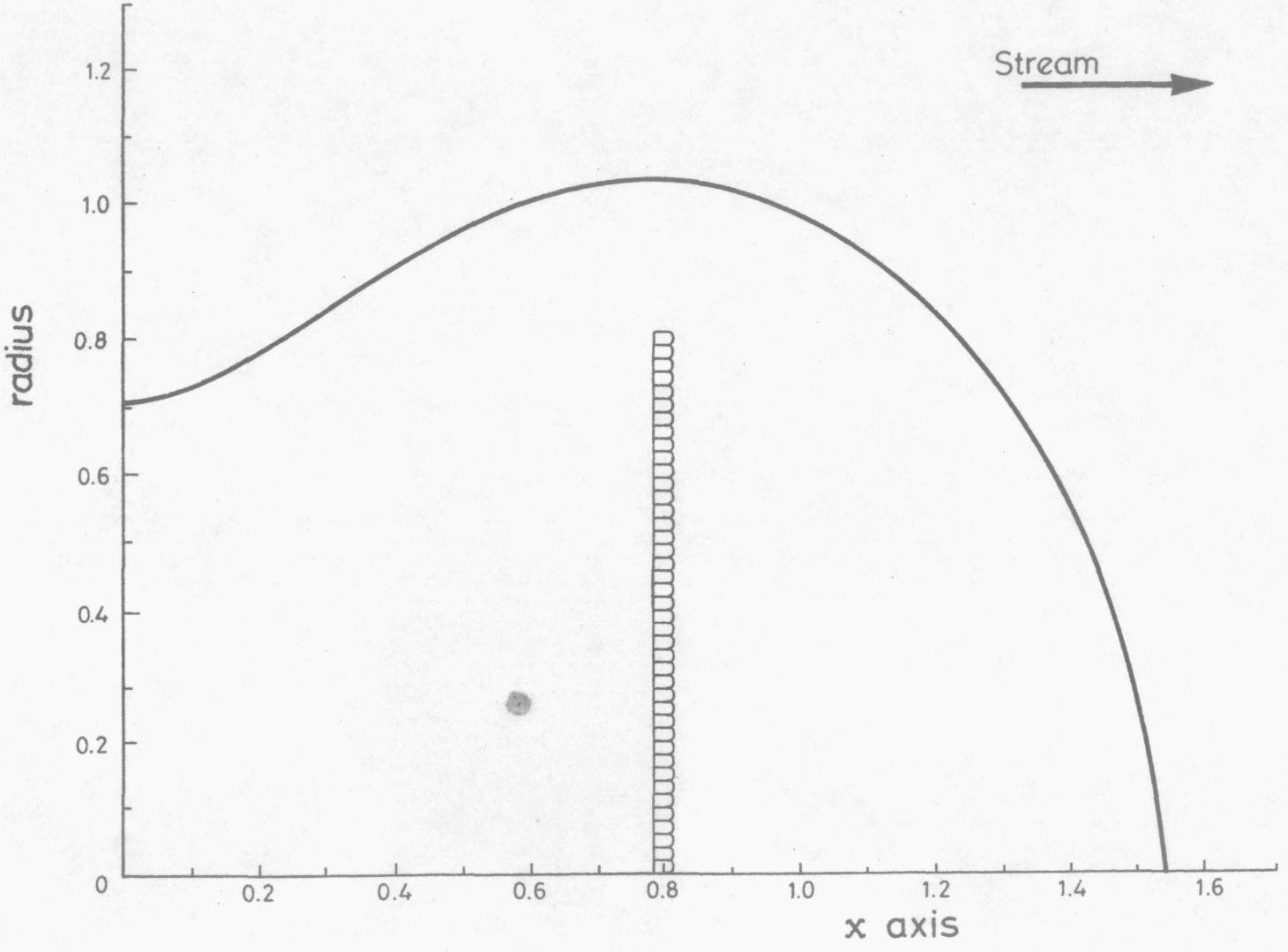

Figure 5. Two type B discs. $\xi = -0.8, 0.8$, $f_o = 2.5$, $\eta_1 = 0.8$

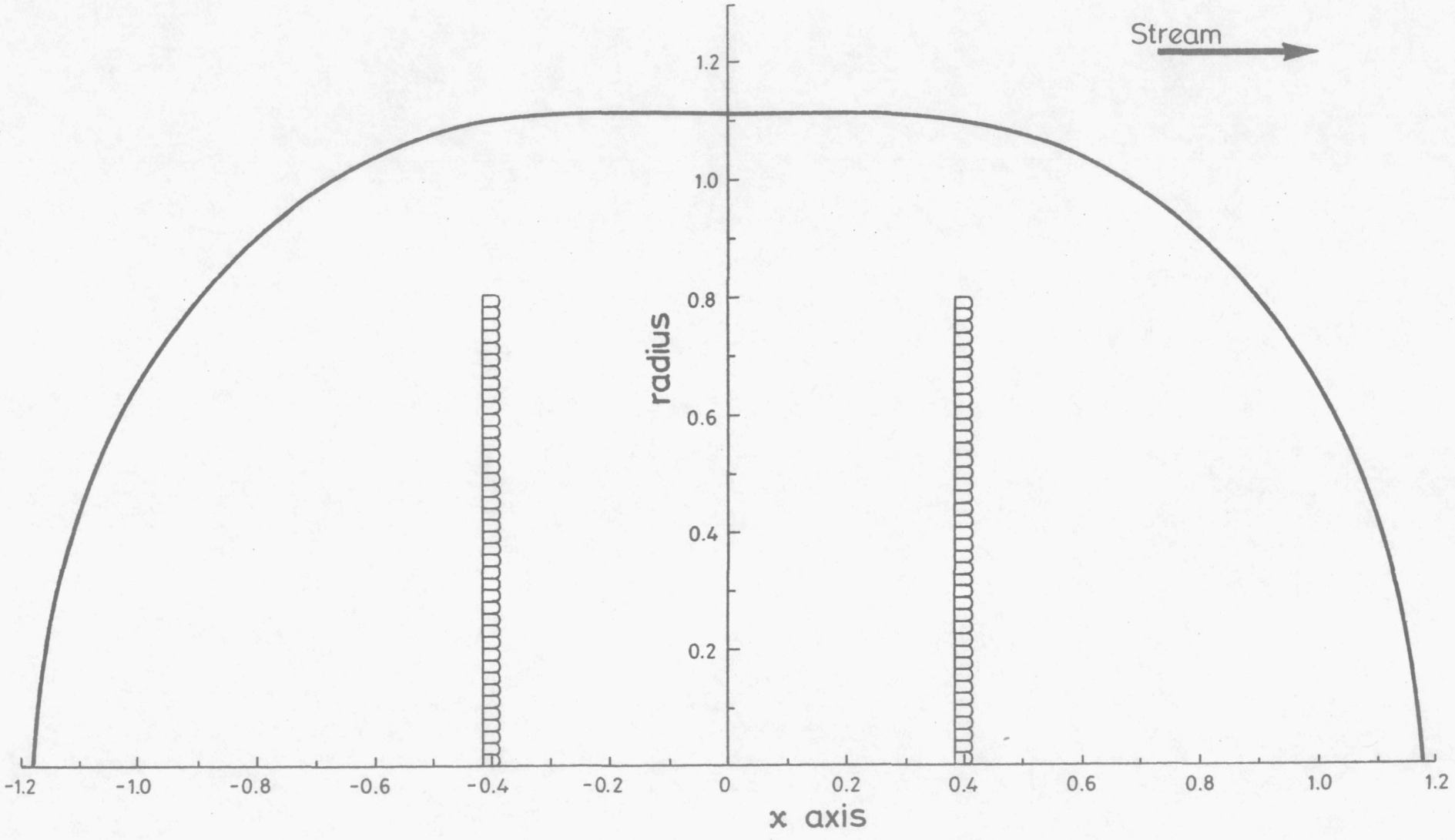

Figure 6. Two type B discs. $\xi = -0.4, 0.4$, $f_o = 2.5$, $\eta_1 = 0.8$

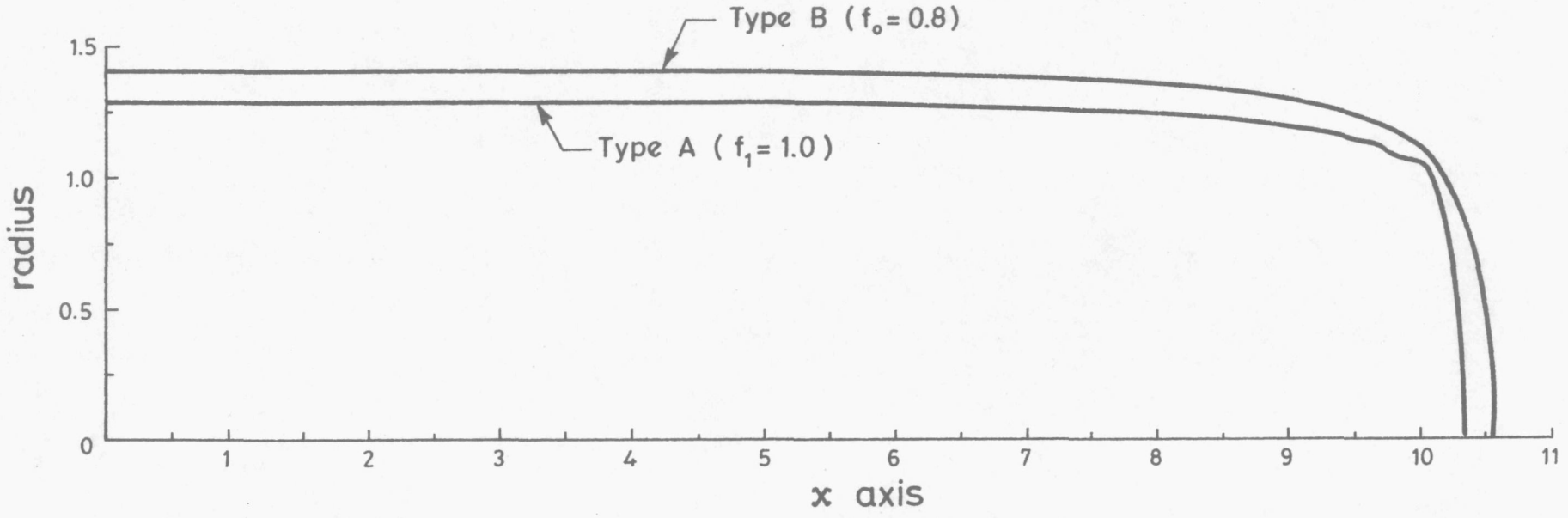

Figure 7. Comparison between bodies generated by type B and type A source discs. (η_1=1.0 , $\Delta\xi$ = 0.4 over $-10 \leq \xi \leq 10$)

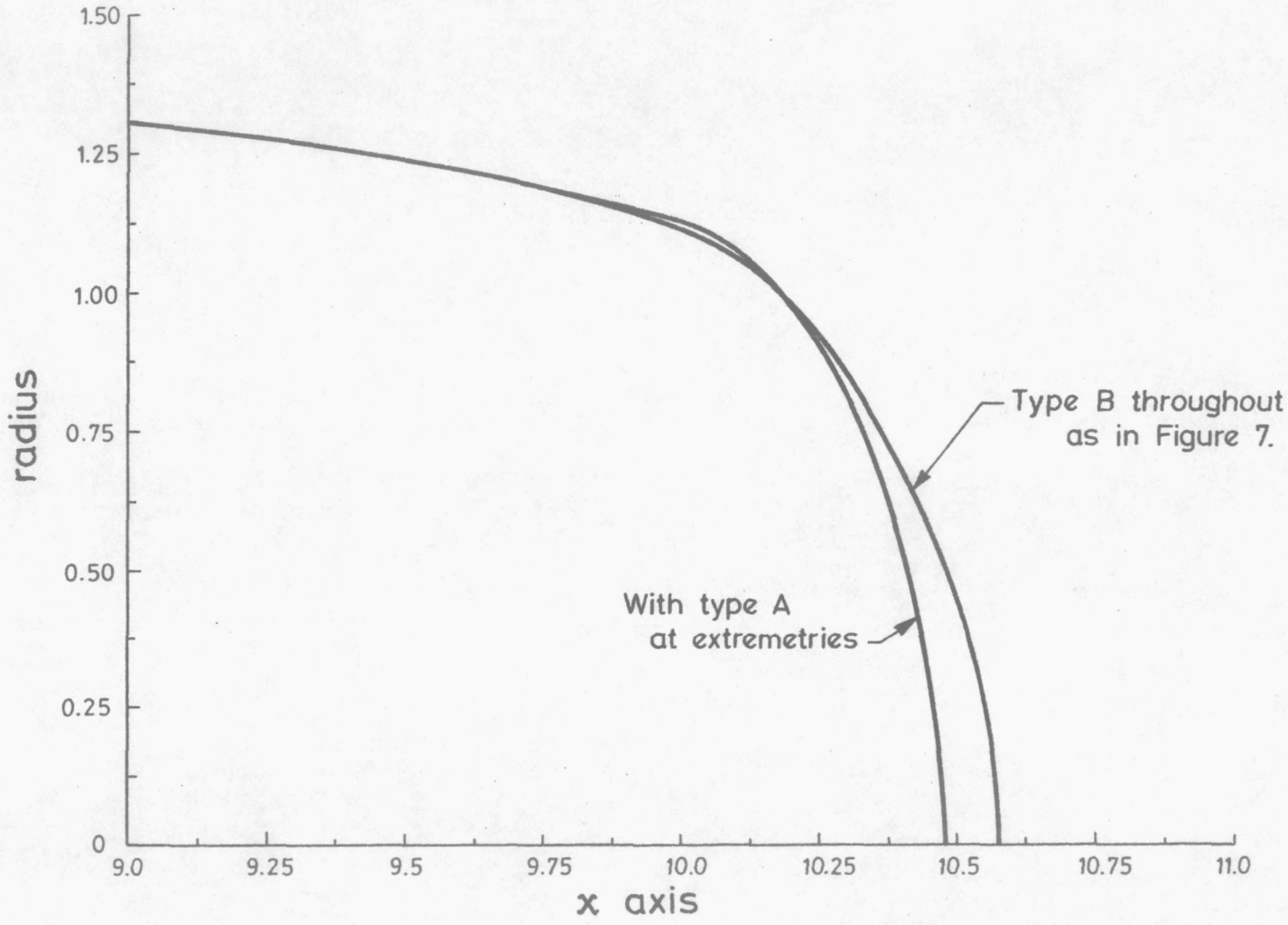

Figure 8. Nose blunting produced by type A discs at extremities.
(Type A discs at $\xi = -10$ and 10 , $f_1 = 1.2$, $\eta_1 = 1.0$)

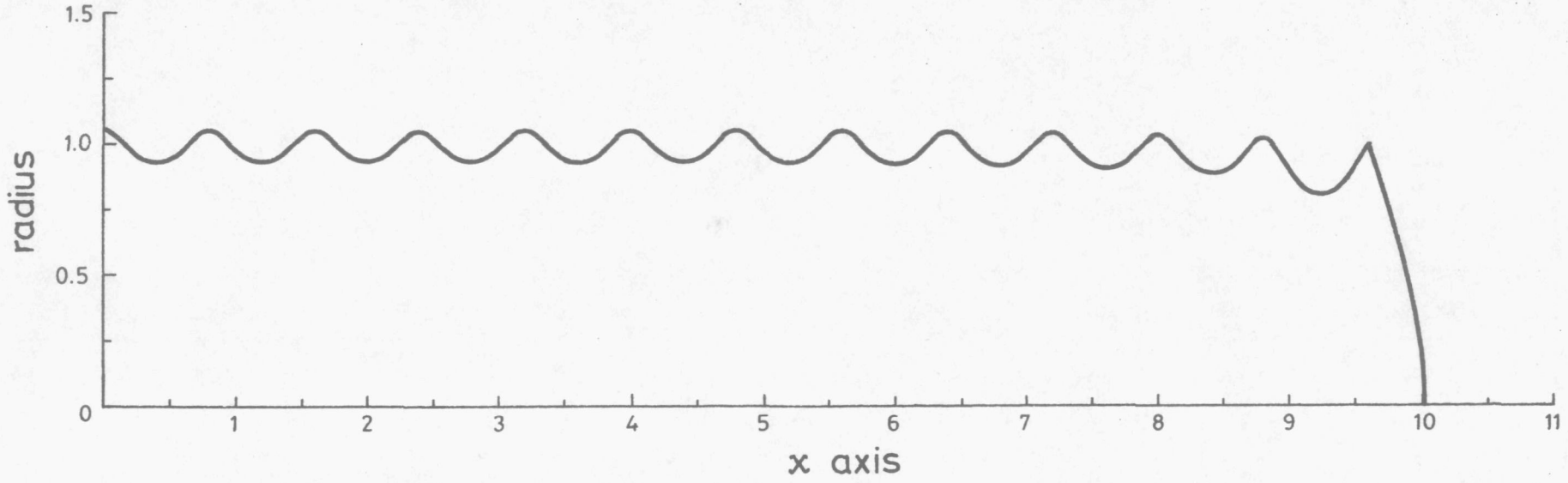

Figure 9. Surface ripples caused by having too great a disc spacing.
($\eta_1 = 1.0$, $f_o = 0.8$, $\Delta\xi = 0.8$ over $-10 \leqslant \xi \leqslant 10$)

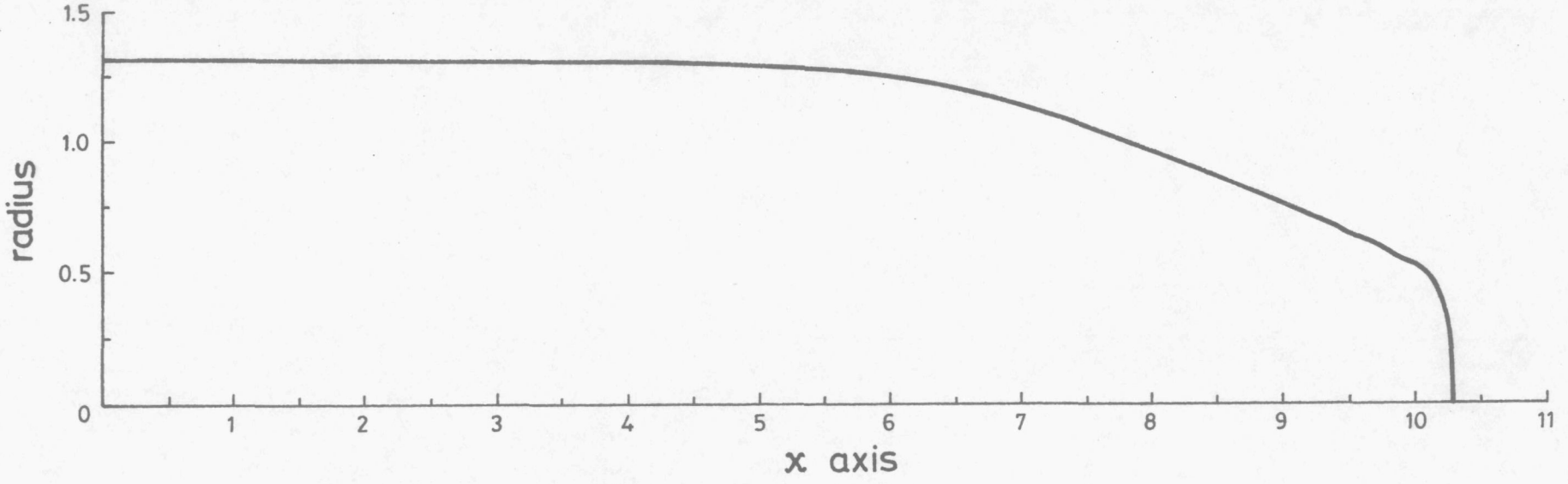

Figure 10. A body having a tapered blunt nose.

$|\xi| \leq 6.0$, $\Delta\xi = 0.4$, $f_o = 0.7$, $\eta_1 = 1.0$, Type B

$6.0 \leq |\xi| \leq 9.6$, $\Delta\xi = 0.4$, $f_o = 0.75$, $\eta_1 = 1.0 - 1/6(|\xi| - 6.0)$, Type B

$|\xi| = 10$, $f_1 = 1.2$, $\eta_1 = 0.4$, Type A

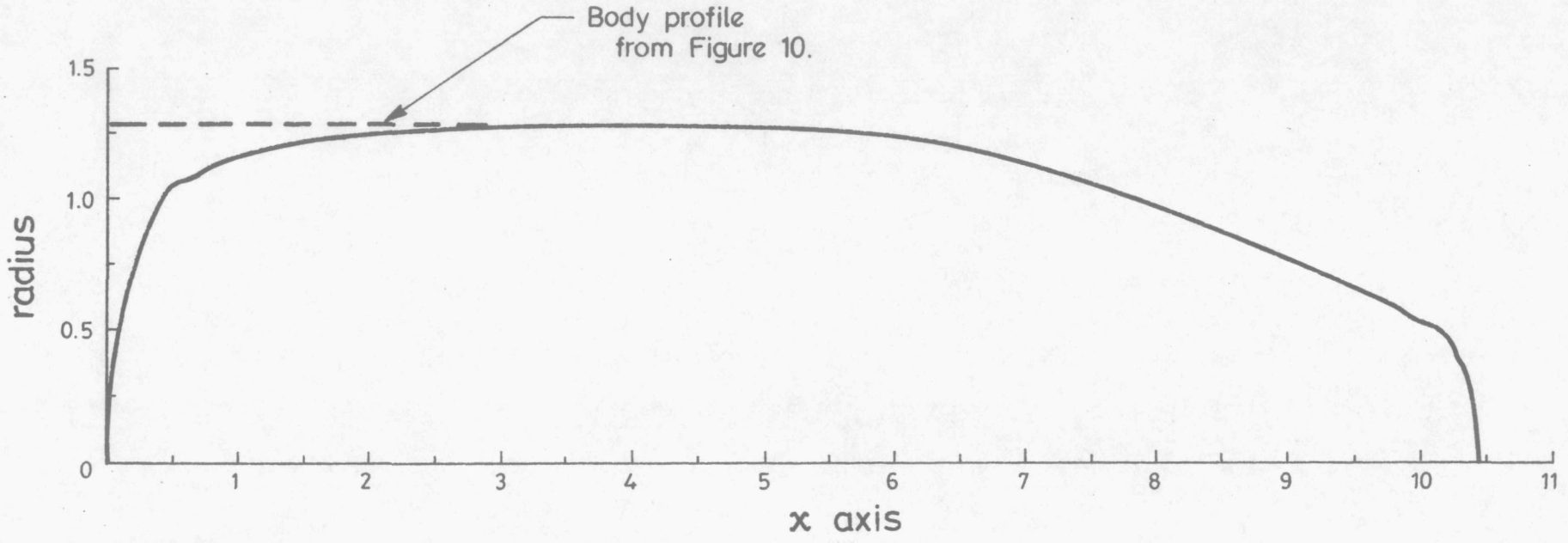

Figure 11. A body which is not symmetric in the x sense.

$0 \leqslant \xi \leqslant 6.0$, $\Delta\xi = 0.4$, $f_o = 0.7$, $\eta_1 = 1.0$, Type B

$6.0 \leqslant \xi \leqslant 9.6$, $\Delta\xi = 0.4$, $f_o = 0.75$, $\eta_1 = 1.0 - 1/6\,(\xi - 6.0)$, Type B

$\xi = 10$, $f_1 = 1.2$, $\eta_1 = 0.4$, Type A

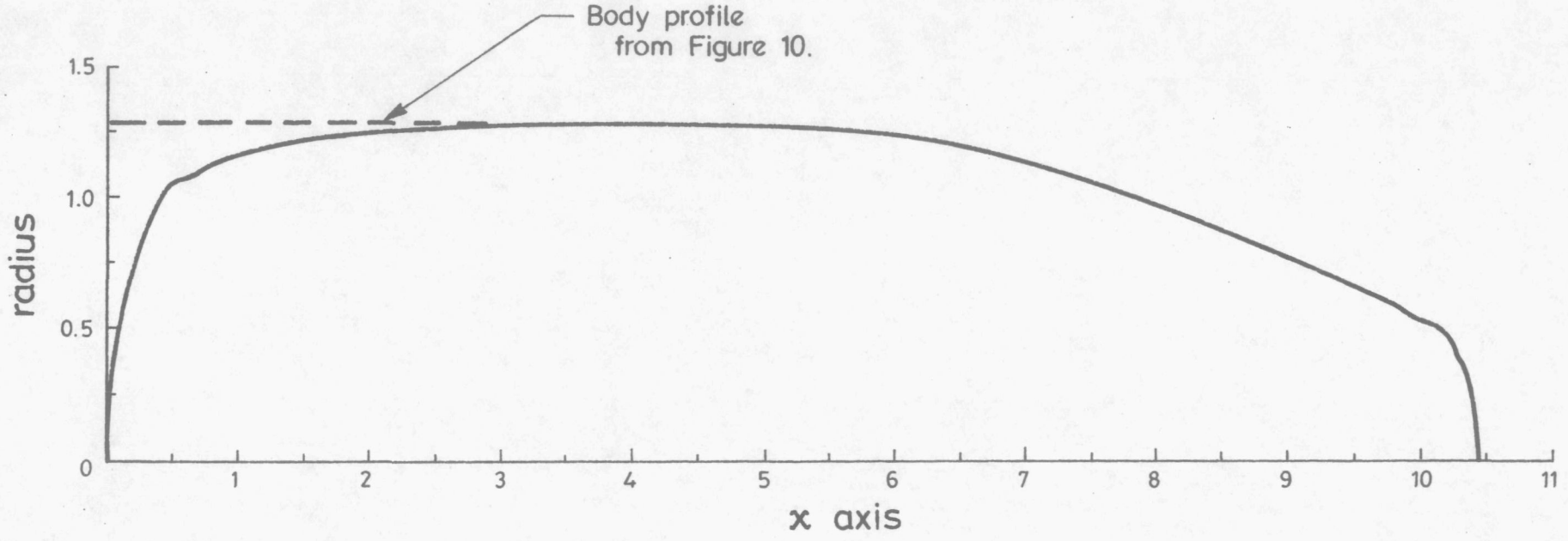

Figure 11. A body which is not symmetric in the x sense.

$0 \leqslant \xi \leqslant 6.0$, $\Delta\xi = 0.4$, $f_o = 0.7$, $\eta_1 = 1.0$, Type B

$6.0 \leqslant \xi \leqslant 9.6$, $\Delta\xi = 0.4$, $f_o = 0.75$, $\eta_1 = 1.0 - 1/6\,(\xi - 6.0)$, Type B

$\xi = 10$, $f_1 = 1.2$, $\eta_1 = 0.4$, Type A